

III. METHODOLOGY

To detect LFIA, we utilize digital sensors embedded near the protected circuitry (AES in this paper) on the chip. Laser illumination alters the voltage level of the targeted gate and propagates an IR drop in the surrounding area. This IR drop, caused by I_{PGN} , reduces the voltage level near the laser target, as modeled in the RC circuitry shown in Fig. 1. In the absence of a laser attack, the effective voltage supplied to the circuit is approximately $Vdd_b \approx Vdd$, neglecting I_d from circuit activity for simplicity. However, under laser illumination, this voltage decreases to $Vdd_{b(faulty)} \approx Vdd - R \times I_{PGN}$. Indeed by leveraging digital sensors, this IR drop can be detected as it induces a voltage drop ($R \times I_{PGN}$) in the circuit's power supply. To ensure effective detection, the DS should be placed close to the laser impact area, i.e., near the AES core. This voltage drop lowers the DS voltage and causes variations in its FN value.

To design an LFIA detector resilient to temperature changes, we monitor the differential FN values across consecutive clock cycles. If this difference exceeds a threshold TH , an alarm is raised. However, due to the FPGA implementation of DS and the nature of analog signals, FN values differ between even and odd clock cycles because of variations in the rise and fall propagation times of the delay chain input (a_0 in Fig. 1). To address this, FN in each clock cycle CC_i (FN_i) is compared to FN_{i-2} . Using Eq. (1), the sensor raises an alarm at time i if the threshold TH is crossed. Namely:

$$Alarm = \begin{cases} 1 & \text{when } FN_{i-2} - FN_i \geq TH, \\ 0 & \text{otherwise.} \end{cases} \quad (1)$$

In this paper, we implemented three sensors alongside the AES module on the Digilent Nexys Video board and used a real laser setup to inject faults into the AES hardware core. To demonstrate that laser illumination generates a propagated IR drop, the first sensor, $S1$, was placed and routed within the AES logic, the second, $S2$, was positioned moderately far from the AES, and the third, $S3$, was placed completely away from the laser shot spot in another zone of the target FPGA while the sensor threshold TH for detecting fault is set to $TH = 2$.

IV. EXPERIMENTAL RESULTS

A. The Effect of Laser Illumination on Sensors

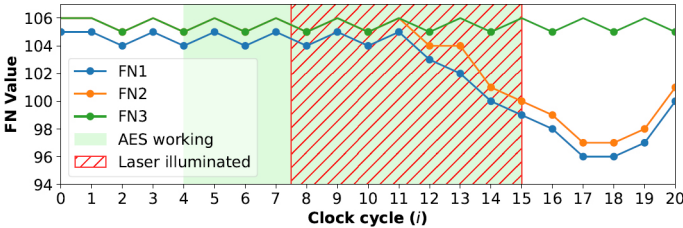


Fig. 3: Variation of FN over time for a laser illumination with 150 ns duration and 1,632 mW power when targeting AES core.

The first set of results shows the variation in the outcomes of the three embedded sensors ($FN1$, $FN2$, and $FN3$) over time when the AES core is active, and laser illumination is applied. As shown in Fig. 3, the green area (clock cycles 4 to 15) indicates AES activity, while the red-striped area (clock cycles 7.5 to 15, $7.5 \times 20 \text{ ns} = 150 \text{ ns}$) represents laser illumination. Before the laser illumination, $FN1$ fluctuates between 104 and 105, while $FN2$ and $FN3$ remain 1 unit higher due to $S1$'s closer proximity to AES. This fluctuation is due to slight

propagation delay differences along the sensor line. During laser illumination, a significant IR drop causes $FN1$ and $FN2$ to decrease, while $FN3$, located in a different FPGA region, remains unaffected. Although $S2$ is farther than $S1$ from the laser spot, it is still influenced by the induced IR drop unlike $S3$ which experiences negligible impact.

B. Detectability with Multi Sensor Integration

In this analysis, we assess the detectability of three embedded sensors under laser attacks (with pulse duration of 150 ns, power of 1632 mW, and at 1,064 nm wavelength). Fault injection tests on the FPGA AES module yielded 1155 faults.

Table I highlights the detection rate of the sensors. Sensor $S1$ achieves an overall detection rate of 87.27%. Sensor $S2$ performs similarly but slightly lower detection rate (85.88%) due to its farther proximity to the target. Sensor $S3$, being farthest, has minimal detectability (1.12%) as it cannot sense the propagated IR drop. We conclude from these experiments that combining $S1$ and $S3$ effectively detects faults while minimizing false alarms caused by noise, such as voltage fluctuations, as faults affect only one sensor while noise alters both. We will dig into such details in our future work.

TABLE I: Fault Detection and Detection Rates by all sensors

Total Faults	Detected Faults			Detection Rate (%)		
	S1	S2	S3	S1	S2	S3
1155	1008	992	13	87.27	85.88	1.12

V. CONCLUSION AND FUTURE DIRECTIONS

We proposed a lightweight TDC-based scheme to detect LFIA by sensing laser-induced IR drops. Testing on a AMD/Xilinx Artix-7 FPGA showed that the IR drop propagates to neighboring circuits and decreases with distance from the laser spot. Thus, TDCs should be placed near areas likely targeted by adversaries. Meanwhile to decrease the false alarm rate we also benefit from the sensors placed far from the target. Our results demonstrate a detectability rate of 87%. The method is portable to other FPGAs, ASICs, and PDKs, and is robust against temperature and voltage changes thanks to its differential design. Future work will explore the impact of device aging and noise from neighboring logic, as well as examine quantitatively whether employing multi-sensor systems can enhance fault detection performance by reducing both false alarms and missed detections.

ACKNOWLEDGEMENTS

This work was supported by the National Science Foundation CAREER Award (NSF CNS-1943224). This work has partly benefited from the bilateral MESRI-BMBF project "APRIORI" from the ANR cybersecurity 2020 call.

REFERENCES

- [1] X. Wang et al., "A Correlation fault attack on rotating S-Box masking AES," in *Asian HOST*, 2021, pp. 1–6.
- [2] S. Guilley and J.-L. Danger, "Global faults on cryptographic circuits," in *Fault Analysis in Cryptography*. Springer, 2012, pp. 295–311.
- [3] H. Wei et al., "Cheap and cheerful: A low-cost digital sensor for detecting laser fault injection attacks," in *SPACE*, 2016, pp. 27–46.
- [4] M. Anik et al., "On-Chip Voltage and Temperature Digital Sensor for Security, Reliability, and Portability," in *ICCD*, 2020, Hartford, CT, USA.
- [5] M. Ebrahimabadi et al., "DELFINES: Detecting laser fault injection attacks via digital sensors," *TCAD*, vol. 43, no. 3, pp. 774–787, 2023.
- [6] A. H. Johnston, "Charge generation and collection in PN junctions excited with pulsed infrared lasers," *Trans. Nucl. Sci.*, vol. 40, pp. 1694–1702, 1993.
- [7] R. A. C. Viera, "Simulating and Modeling the Effects of Laser Fault Injection on Integrated Circuits," Theses, Université Montpellier, Oct 2018.